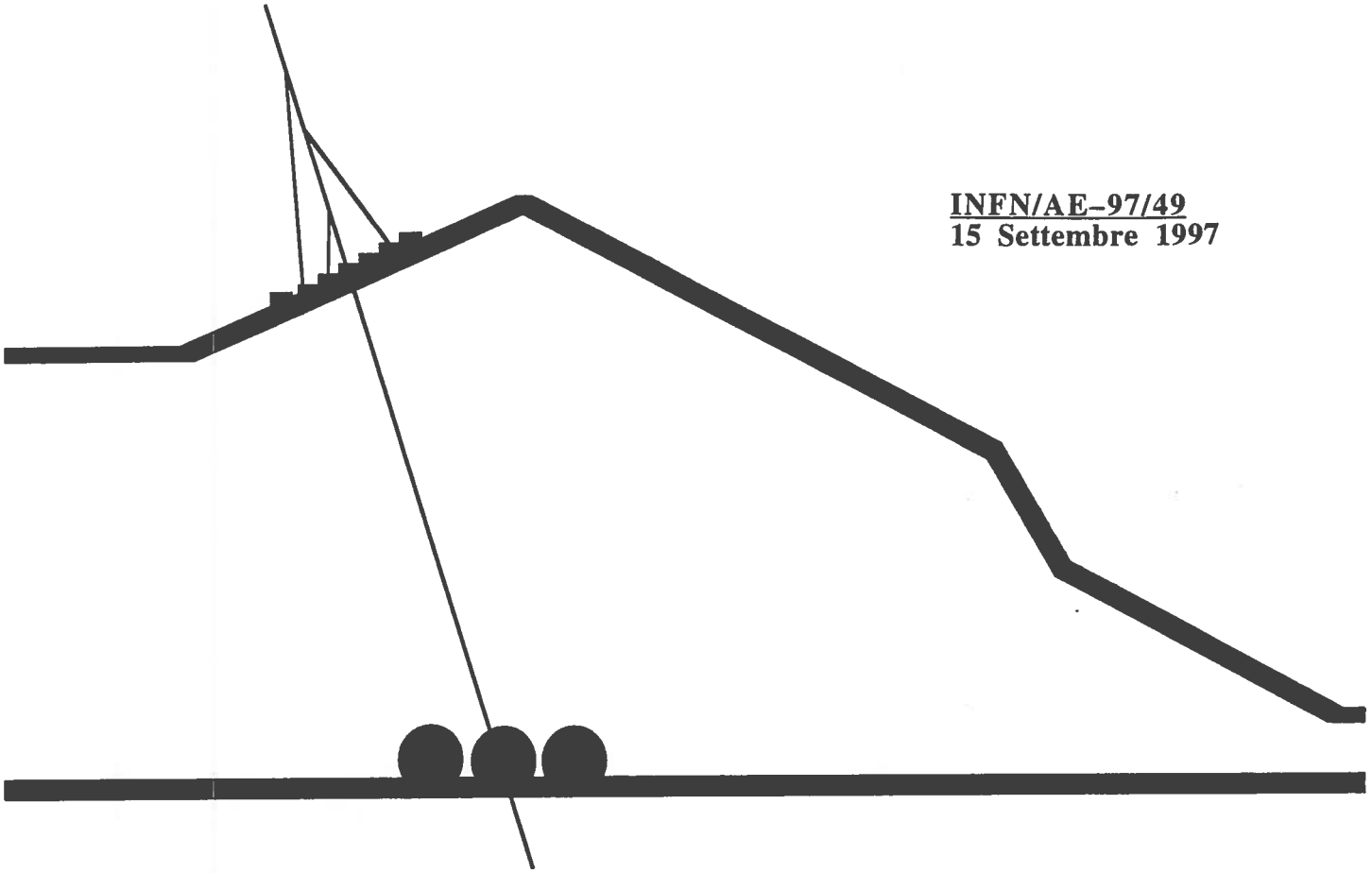

INFN/AE-97/49
15 Settembre 1997

Study of solar neutrino detection in the 600 ton liquid argon ICARUS time projection chamber

R. Dolfini et al.

INFN – Laboratori Nazionali del Gran Sasso

Published by ***SIS–Pubblicazioni*** *dei Laboratori Nazionali di Frascati*

INFN – Istituto Nazionale di Fisica Nucleare
Laboratori Nazionali del Gran Sasso

INFN/AE–97/49
15 Settembre 1997

Study of Solar Neutrino Detection in the 600 Ton Liquid Argon ICARUS Time Projection Chamber

R. Dolfini, M.Maris, C.Montanari, A.Rappoldi, C.Vignoli

Dipartimento di Fisica e INFN, Università di Pavia, via Bassi 6, Pavia, Italy

A.Borio di Tigliole, A.Cesana, M.Terrani

CESNEF Politecnico di Milano e INFN, Via Ponzio 34/3 (Mi), Italy

F.Cavanna, G.Nurzia

Dipartimento di Fisica e INFN, Università dell'Aquila, via Vetoio, Coppito (AQ), Italy

F.Pietropaolo

Dipartimento di Fisica e INFN, Università di Padova, via Marzolo 8, Padova, Italy

Abstract

The ICARUS detector offers the unique possibility to derive for the first time sound information on the ^8B neutrino energy spectrum. The main problem of the solar neutrino detection arises from the environmental radioactivity. We study the topology and the frequencies of the events induced by the radioactivity of the rocks in a 600 ton detector located in the hall C of the underground Gran Sasso Laboratories. With a convenient choice of the neutron shield and of the off-line triggers, the frequency of spurious events can be reduced to a level compatible with the solar neutrino detection.

1. Introduction.

The ICARUS search programme [1], deals with explicit neutrino oscillations at long and medium baselines. with a proton decay experiment and with a neutrino observatory at the Gran Sasso laboratory (LNGS). The different items imply different liquid argon sensitive masses. An intermediate detector [2] is the necessary step in order to test the main technical solutions and to gain in situ experience for what concerns the handling of the apparatus: safety, LAr supply, reliability of TPC mechanical components and electronics, etc. Such a detector can also give significant information about some important physics items, among which, the measurement of the solar neutrinos energy spectrum. A 600 ton module has a mass close to that of the Kamiokande detector, but the higher efficiency, the better energy resolution, and the much more detailed description of each event offer the unique possibility to derive for the first time sound information on the ^{8}B neutrino energy spectrum. Therefore, in a reasonable data collection time, definite conclusions about some of the open solar neutrino problems could be reached. The energy associated to solar neutrino interactions is very low so that natural background interference is expected. The aim of the present work is the study of the topology of the events induced by the radioactivity of the rocks and of their frequency in a 600 ton detector located in hall C of the underground Gran Sasso Laboratories. It will be shown that, with a convenient choice of the neutron shield and of the off-line triggers, the weight of spurious events can be reduced to acceptable values. The programs used for the simulations were GEANT and MCNP [3].

2. Simulation geometry

LNGS hall C and ICARUS detector have been simulated according to the scheme displayed in fig. 1. The hall is a parallelepiped 20.6 m wide, 9 m high and 100 m long, surmounted by a half cylinder 10.3 m of radius. The detector is an iron parallelepiped, located in the corner near the main entrance of the hall. The volume (7.3 x 3.7 x 18 m^3), is completely filled with liquid argon, and is " seen" by four vertical TPC's (1.6 drift length, 3.7 m high, 18 m long). The resulting sensitive volume is about 255 m^3, corresponding to 360 ton Lar. For the time being, the dewar walls are assumed to be made of stainless steel 4 cm thick. The dewar is surrounded by a closed space, 0.6 m thick, filled with a low density material for thermal insulation and by a neutron shielding layer containing both a neutron moderator and a neutron absorber.

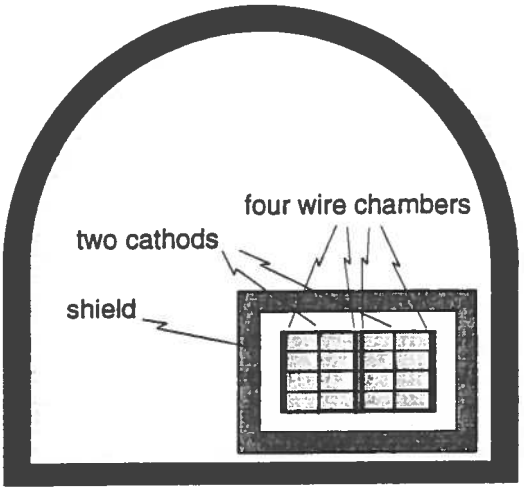

Transversal view

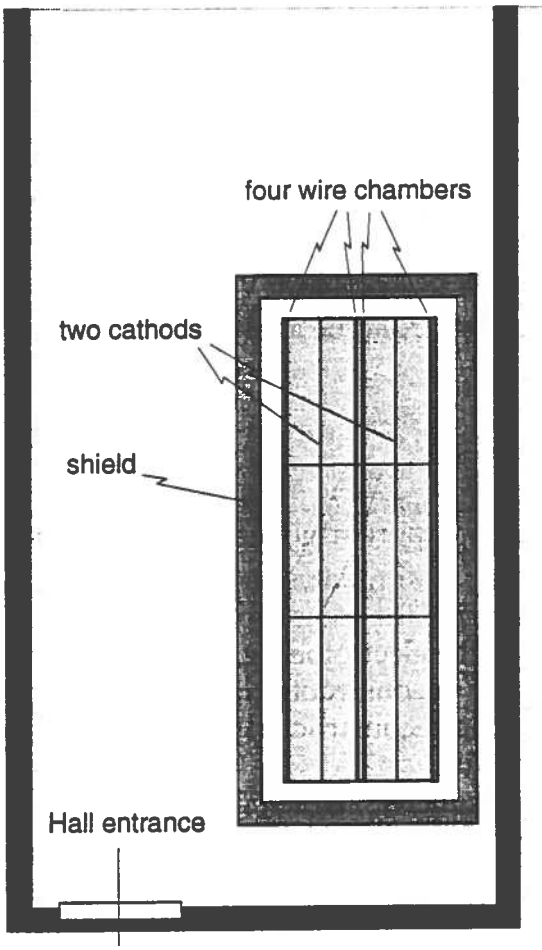

Longitudinal view

Fig 1 Schematic representation of hall C and ICARUS detector

3. Solar neutrino interactions

Interacting with argon atoms, solar neutrinos can produce energetic electrons by elastic ν-e scattering or nuclear absorption.
The later consists essentially of two processes: the super allowed Fermi transition to the 4.38 MeV ($J^{\pi} = 0^{+}$, T = 2) isobaric analogue state of ^{40}K and the allowed Gamow-Teller transitions [4] to several low lying states ($J^{\pi} = 1^{+}$, T=1) mainly between 2.73 and 3.80 MeV. The primary electron is accompanied by a number of photons generated by Bremsstrahlung or emitted in the de-excitation of ^{40}K nucleus which can in turn generate secondary electron tracks. Hence, in general, an event consists of a number of electron tracks confined to a relatively small volume of the detector. In practice, the most energetic among these tracks can be supposed to correspond to the primary electron whose energy and initial direction should be accurately measured. The direction constraint is important for the rejection of spurious signals, since in each of the interactions considered there exists a correlation between the incoming neutrino and the out-coming electron. Owing to the presence of background and to the difficulties connected with the reconstruction of low energy electrons tracks, there exists a threshold energy, E_{Th}, below which the information on the direction may be lost. This limits the portion of solar neutrinos which can be measured with our detector. The ^{8}B energy spectrum reaches 14 MeV and the Q value for absorption reactions is 1.5 MeV. Therefore the energy ranges of neutrinos which give rise to detectable electron tracks are:

$E_{Th} \leq E_{\nu} < 14$ (MeV) for elastic events,
$E_{Th} + Q + 2.29 \leq E_{\nu} < 14$(MeV) for Gamow-Teller events,
$E_{Th} + Q + 4.38 \leq E_{\nu} < 14$ MeV for pure Fermi events.

The value of E_{Th} is deduced from the analysis of Montecarlo events.

3.1 Event simulation

The GEANT Montecarlo program generates the neutrinos and the electrons produced in the detector. It simulates the transport of γ's and electrons inside the liquid argon, transforms the ionisation energy into the collected charge on single wires, reproduces the electronic signal by adding the noise, performs a fit of the signal and finally reconstructs the position and the energy from the parameters of the fit. The reconstructed events have been processed with an interactive graphic program.
The following project parameters, which were discussed in ref [1,2], were used:

a) a sensitive mass of 360 tons of liquid argon
b) three sense wire planes put at 60° from one another
c) a wire pitch of 3 mm,
d) an electronic noise, gaussian distributed.

One Montecarlo event is shown in fig. 2. It is characterised by the track of the primary electron generated in the interaction, surrounded by a number of secondary tracks. The choice of the threshold energy for the detection of these secondary electrons is strongly correlated with the electronic noise and with the

sense wire stepping. In our simulation we chose 0.3 MeV. In the following we will call "associated multiplicity" (m) the number of tracks accompanying the electron and "associated energy" (E) the sum of their energies. The simulation shows that the probability of finding these secondary electron tracks vanishes 50 cm away from the interaction point.

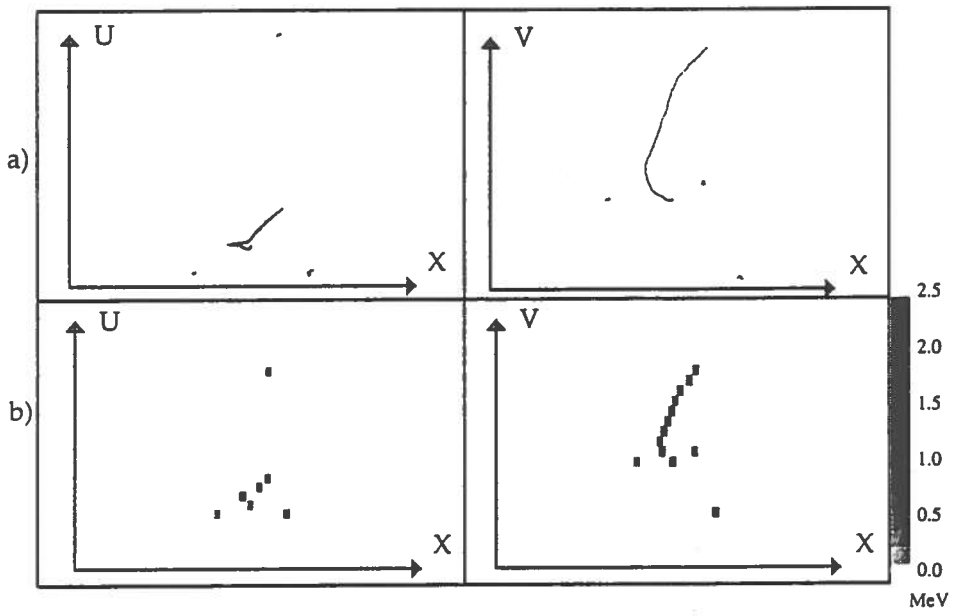

Fig. 2 a) Absorption event as generated by the GEANT Montecarlo program in two wire planes (U and V coordinates) put at an angle of 60°, the x axis is the drift coordinate. b) In the bottom it is shown the same event after digitisation. The grey scale of each pixel is proportional to the deposited charge. The resolution in the horizontal axis (drift direction) is 0.1 mm, and in the vertical axis is 3 mm (wire pitch). The projected track length is about 3 cm, the main electron energy is 7 MeV, the associated energy is 2 MeV and the associated multiplicity is 3.

The electrons tracks are strongly affected by multiple scattering and Bremsstrahlung. The deviation from linearity decreases as the electron energy increases and, in the majority of cases, for energies greater than 5 MeV it is possible to reconstruct at least the track direction.
That's why, for both scattering and absorption events, the energy threshold for the primary electron detection, E_{Th}, was set at 5 MeV. In summary the signature of a solar neutrino interaction is an electron track with energy greater than 5 MeV eventually associated to lower energy tracks contained in a 50 cm radius sphere around it.
In what follows we give a schematic classification of the event topologies resulting from simulations. The correlation between secondary electrons multiplicity and energy will be used to define the off-line triggers and to evaluate the trigger efficiencies $\alpha_{elastic}$, α_{GT} and α_F for scattering or absorption channels.

3.2 Elastic scattering :

$$\nu_{e,\mu,\tau} + e^- \rightarrow \nu_{e,\mu,\tau} + e^-$$

The electron produced via an elastic scattering has an angular distribution strongly picked in the forward direction [5a]. In Fig. 3 the fraction of the elastically scattered electrons (E > 5 MeV) surviving the cut on the angle between the reconstructed electron and the parent neutrino direction is shown. For instance if one choose a direction contained in a 25° cone around the sun/detector direction, the angular efficiency is 65%.
The average number of tracks produced via Compton or pair interaction by the Bremsstrahlung photons associated to the elastic scattered electron is <m>=0.25.

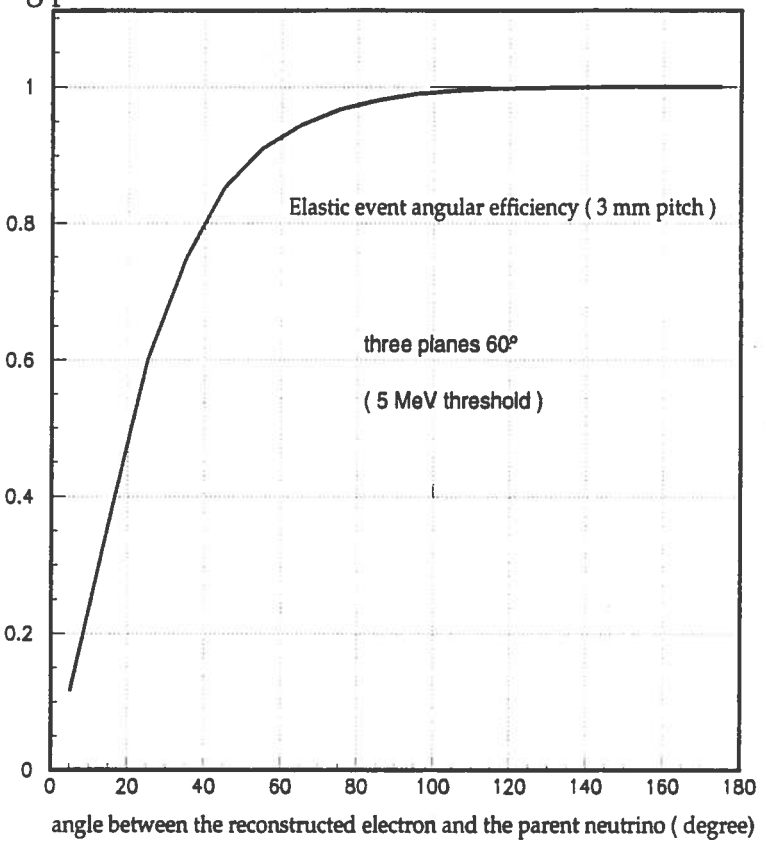

Fig. 3 Fraction of the elastic events as a function of the cone angle within which the reconstructed electron direction in space is contained; the cone axis is defined by the parent neutrino direction.

The fraction of the elastic scattering events as a function of the associated multiplicity (m) and energy (E) is shown in Table I.

	m=0	m=1	m=2	m=3
E ≥ 1 MeV	0	0.034	0.046	0.004
E <1 MeV	0.813	0.099	0.004	0

Table I: Fraction of the elastic scattering events as a function of the associated energy (E) and multiplicity (m). The data obtained after digitisation are used.

3.3 Absorption events :

$$\nu_e + {}^{40}Ar \rightarrow {}^{40}K^* + e^-$$

The angular distributions of electrons [5a] exhibit a broad peak at about 120° or 60° for the Gamow-Teller or Fermi events respectively, but the measured distributions are flattened because of the digitisation, so that, to a first approximation electron tracks directions can be considered isotropically distributed.

a) allowed Gamow-Teller transitions: in Table II the correlation between the associated multiplicity and secondary electrons total energy is shown. The mean number of tracks produced in coincidence with the diffused electron is <m>=1.7.

	m = 0	m = 1	m = 2	m ≥ 3
1≤ E	0	0.178	0.348	0.166
0≤ E <1 MeV	0.052	0.198	0.058	0

Table II: Fraction of the Gamow-Teller events as a function of the associated multiplicity and energy. The data obtained after digitisation are used.

b) super allowed Fermi transition: in Table III the correlation between the associated multiplicity and energy is shown. The Compton mean number produced in coincidence with the diffused electron is <m>=3.2.

	m = 0	m = 1	m = 2	m ≥ 3
E ≥ 1 MeV	0	0.021	0.221	0.705
E <1 MeV	0.004	0.028	0.019	0.002

Table III Fraction of the pure Fermi triggers as a function of the associated multiplicity and energy. The data obtained after digitisation are used.

4. Background events simulation

These computations were performed by MCNP program. The detector was divided in: the external shielding layer, the empty cavity wall 60 cm thick, the iron skin of the dewar and 48 identical cells which fill the LAr sensitive volume of the four TPC which "see" the detector. Scope of the computations was to derive the frequency and energy distribution of background electron tracks in each TPC.

The shielding which surrounds the detector is an array of polyethylene tubes filled with a saturated boric acid aqueous solution. Its thickness is 140 cm over the top and 70 cm along the other sides of the detector.

4.1 Background sources

The following background sources were considered.

a) Natural radioactivity in the hall. The radioactive decay of ^{40}K, uranium, thorium, radon and daughters, present in the rock or in the atmosphere surrounding the detector, can generate photons or neutrons by spontaneous fission (SF) or (α,n) reactions.

The rock surrounding the cavern is assumed to be limestone [6] with a mean density of 2.8 $g \cdot cm^{-3}$, a potassium concentration of 0.33% [7], and an uranium and thorium specific activity of 1.7 and 1.9 $Bq \cdot kg^{-1}$ respectively [8].

From ^{40}K decay 1.46 MeV photons are produced at a rate of 3250 $\gamma/(s \cdot$ kg of natural potassium), and, supposing U and Th chains at the equilibrium, 1.98 photons and 2.48 photons are emitted respectively for each U and Th disintegration. The energy spectrum of these photons extends up to 2.6 MeV.

Considering the radioactive nuclides concentrations quoted above we expect that about $2 \cdot 10^7$ $s^{-1} \cdot kton^{-1}$ photons of various energies be generated in the rock. Photons can also be produced by neutron capture in the rock but in an amount several orders of magnitude lower.

Among natural nuclides SF is important only for ^{238}U. Assuming for uranium the specific activity quoted above, $T_{1/2}(SF) = 8.2 \cdot 10^{15}$ y, $T_{1/2}(\alpha) = 4.5 \cdot 10^9$ y and 2 neutrons per fission [9], we have 1.87 $n \cdot s^{-1} \cdot kton^{-1}$.

In most of the minerals, uranium is present in an oxide form. Hence oxygen is probably the main element involved in neutron production by (α,n) reactions. Assuming that uranium be at the equilibrium with 7 daughters and thorium with 5 daughters alpha emitters, and that all these nuclides have the same neutron yield: $6.5 \cdot 10^{-8}$ n/α–particle [10], we have 1.63 $n \cdot s^{-1} \cdot kton^{-1}$.

In addition to the natural radioactivity, the high energy muons which penetrate the rock, can induce nuclear photo dissociation. The neutron production by this way was estimated to be about $9 \cdot 10^{-3}$ $n \cdot s^{-1}$ $kton^{-1}$ [1b]. Since this figure about two orders of magnitude lower than the previous ones this way of production is relatively unimportant.

b) Radioactive pollution in liquid argon. Natural argon probably contains small amounts of ^{39}Ar and ^{42}Ar. The second, which is by far the most important source of background, is supposed to be present with a concentration of $7 \cdot 10^{-22}$ atoms of ^{42}Ar per natural Ar atom [11]. Recently this figure was experimentally confirmed [12]. However the maximum energy of β-rays emitted in its decay is 3.5 MeV, well below 5 MeV. The statistical error in the energy reconstruction induces the presence of electron tracks over this threshold. Supposing a gaussian distribution of the reconstructed energies with a standard deviation of 12% at most, we obtain about $3 \cdot 10^{-2}$ tracks/day with an isotropic distribution. Taking into account the angular cut-off (25 degree cone around the neutrino direction) they become $1.2 \cdot 10^{-3}$ track/day.

c) Radioactivity of structural materials. Because, at present, the information about the materials to be used in the detector construction is lacking at all, a sound evaluation of the contribution from this source to noise is impossible.

We limit our considerations to stainless steel, which is by now the material proposed for the dewar construction. The results of a radiochemical analysis of various samples of iron and stainless steel performed at LNGS [13], show that very clean materials are commonly offered on sale. For instance in one of the samples, ^{238}U , ^{232}Th, ^{40}K and ^{60}Co were not found, with the following detection limits: 0.01, 0.02, 0.2, 0.02 Bq/kg respectively. In a 150 ton dewar these limits would correspond to: 0.12 g of U (about $2 \cdot 10^{-3}$ SF neutron/s) and $3 \cdot 10^{3}$, $3 \cdot 10^{4}$, $3 \cdot 10^{3}$ Bq of the other radio nuclides.

4.2 Computations

Scope of the computations was to determine the intensity and energy distribution of electron tracks produced in the sensitive volume. Photons and neutrons were considered independently.
Being by far the most important one, the natural radioactivity of the rocks was the only radiation source considered in details. Particular care was devoted to neutrons which are the only radiation able to generate electrons with energy in the interval 5 - 10 MeV, i.e. in the energy range of the solar neutrino events searched for in ICARUS apparatus. The radiation source is supposed to be uniformly distributed in a layer of rock, lining the hall. The probability that a particle, born in the rock, produces some effect in the detector room, decreases obviously with the depth at which it is generated so that in practice the source has a relatively small thickness which depends on the rock composition and the energy spectrum of the emitted radiation. An estimate of this parameter was obtained by evaluating photon and neutron escape probability from spheres of limestone rock of increasing diameter having a point source at the centre. Photon spectrum was that resulting from the nuclide mixture said above while neutron source was supposed to have ^{238}U SF spectrum. This test showed that both kind of radiations, when generated at depths greater than 1 m, have a negligible escape probability. Hence the source was supposed to be uniformly distributed in a layer of rock 1 m thick lining the walls of the hall.
Taking into account the dimensions of the apparatus, one can expect a very low probability that a particle generated in a given point of the source produces one electron into a reasonably small detector volume and energy interval. For this reason in order to obtain a fair statistics within an acceptable computing time, the computation was performed in separate steps.
1:- Starting from the source previously described the photon (or neutron) energy spectrum in various points of the hall surface was computed. The neutron spectrum, calculated in an isolated point of the cavern well apart from the walls and the detector, was used to derive a normalisation factor by comparison with the measured flux [14].
The results were fairly independent of position so that an unique energy spectrum (one for photons and one for neutrons) was adopted in any point of the cavern surface.
2:- A new source (one for each kind of radiation), with these characteristics, was supposed uniformly distributed on the inner surface of the cavern, and used as input for the computation of the γ-fluence in each detector cell.

3:- The γ-ray spectra were used to generate ,in a liquid Ar volume with dimensions greatly exceeding the γ-rays mean free path, the spectrum of electron tracks and to estimate the correlation between the photon fluence and the electron tracks density, i.e. to derive the ratio (track density/γ-ray fluence). Neutron spectra were represented with 22 energy groups between 10^{-10} and 20 MeV, while for electrons and gamma-rays a 14 groups representation between 0 and 10 MeV was chosen. The following results were obtained.

a) Photon background

In the two external TPC chambers $1.8 \cdot 10^5$ electron tracks/day are foreseen. Going to the detector centre the track density decreases by more than one order of magnitude. The mean energy distribution of electron tracks in the detector is shown in Fig. 4. No electron tracks are expected with energy grater than 2.4 MeV. Electron tracks with a greater energy can be simulated because of errors in the energy reconstruction. Assuming the same energy resolution assumed above , the probability that a 2.4 MeV electron simulates a 5 MeV track is less than $3 \cdot 10^{-7}$. Being the integral above 2 MeV about 0.3 % of the total electron spectrum we expect from this source at the most $1.8 \cdot 10^5 \cdot 3 \cdot 10^{-7} \cdot 3 \cdot 10^{-3} = 1.6 \cdot 10^{-4}$ 5 MeV tracks /day/chamber. One third of the tracks exceeds the 300 keV threshold for secondary electrons identification. If we suppose that the time required for the readout of an event is 1 ms, $1.2 \cdot 10^{-3}$ tracks/trigger are expected.

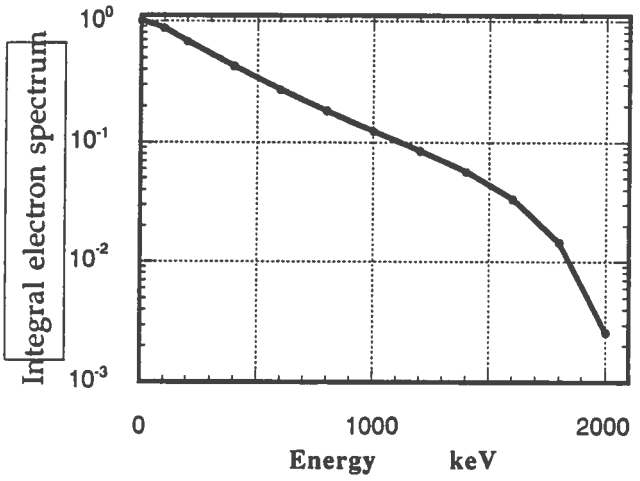

Fig. 4. Integral (E-->∞) electron track spectrum generated from photon interaction

b) Neutron background

The background tracks are generated by photons following thermal neutron capture. Only a small fraction of neutron captures occurs inside the sensitive volume. In the bare detector, neutrons are mainly captured in the iron of the dewar walls. When the detector is surrounded by the shield proposed above most of the captures occur in boron, resulting in a less intense and softer γ-ray

source. The background depression factor depends on energy: in the high energy region, the most important in our case, the factor is greater than 10^3.

The frequency (s^{-1}) of electron tracks (above a given energy) in a TPC is given by:

$$f_E = N_\Phi \cdot F \cdot V \cdot f_\gamma \cdot R_E$$

where N_Φ is the neutron flux normalisation factor, F is the factor between γ-ray fluence and track density, V is the chamber volume, f_γ the mean γ-ray fluence, R_E the fraction of electron tracks above the given energy.

Normalisation factor = measured flux (n/cm^2 sec) [14] / computed fluence (n/cm^2) = 87 s^{-1} = 7.52 10^6 day^{-1}.
Electron track density (cm^{-3})/γ-ray fluence (cm^{-2}) = 0.097 cm^{-1}.
Chamber fiducial volume = 0.65 10^8 cm^3.
The mean γ-ray fluences obtained in each TPC are listed in the first row of Tab. IV and the electron tracks integral distribution is shown in Fig. 5.

	TPC 1	TPC 2	TPC 3	TPC 4
mean γ-ray fluence	1.5 10^{-12}	7.2 10^{-13}	6.2 10^{-13}	1.4 10^{-12}
R(E>5MeV)	0.0128	0.0062	0.0055	0.007
tracks/day	0.90	0.21	0.16	0.45
R(E>6MeV)	0.0053	0.0008	0.0009	0.0035
tracks/day	0.36	0.02	0.03	0.18

Tab. IV Background electrons track frequency. The four TPC are numbered from left to right looking the dewar from the entrance door.

In the same table it is reported the number of tracks/day with energy greater than 5 MeV (6 MeV), expected in each TPC.

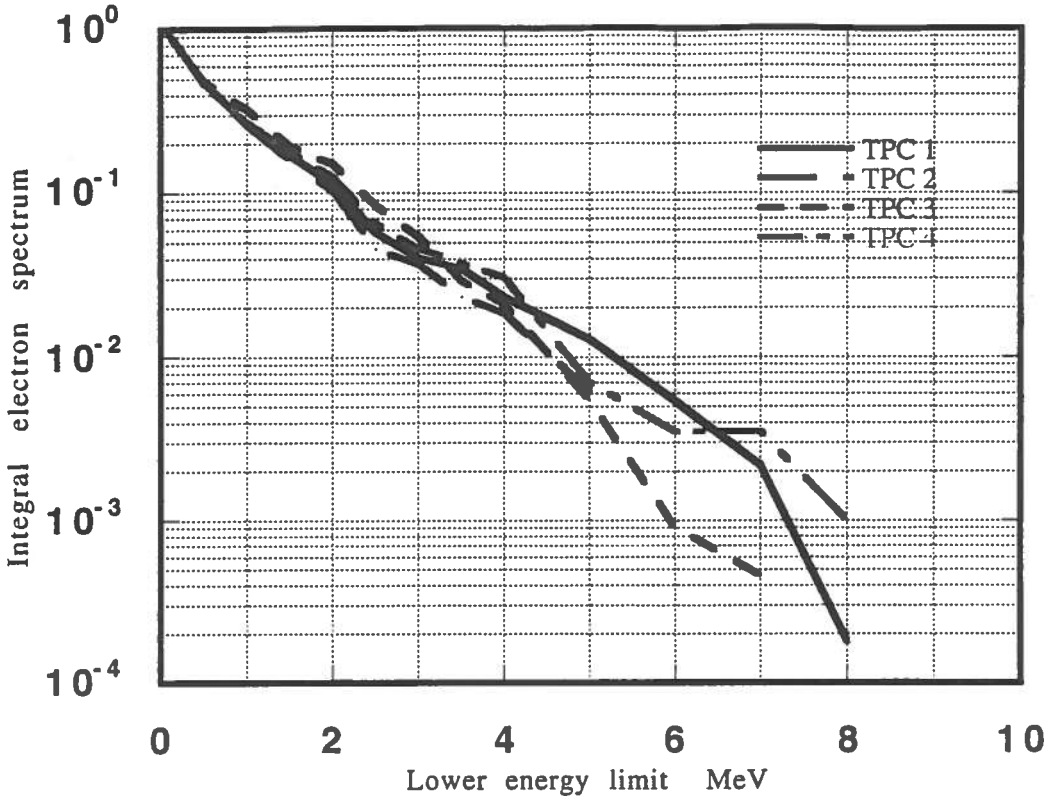

Fig 5. Integral (E-->E_{max}) electron track spectrum generated by neutrons

4.3 Background

Neutrons are by far the first cause of noise. They can generate an electron track with energy greater than 5 MeV, with a frequency just below 1.7 events/day in the whole detector i.e. about 620 events/year. The γ-ray field in the cavern or the γ-rays emitted in the decay of radioactive contaminants (of liquid argon or of the dewar material), which are of comparable importance, do not add a relevant contribution. A little more attention should be deserved to neutron emitted from ^{238}U contamination in the dewar walls. As said above we can expect less than $2\ 10^{-3}$ neutrons/s. These neutrons can be thermalised in practice only in the shield and, only if reflected into the detector, can be captured causing a background event. It is then obvious that their contribution cannot be important. A separate computation showed that their contribution should not exceed 10^{-2} tracks (with energy > 5 MeV) /day.
Because the neutrons are absorbed mainly outside the sensitive volume, the topologies of background and neutrinos elastic scattering events are quite similar. Hence the correlation between the energy and multiplicity associated the noise tracks with $E \geq 5$ MeV is the same shown in Tab. I.

5. Events trigger and background results

From the results reported in reference [1] about 330 elastic scattering events per year, with a 5 MeV kinetic energy cut-off, are expected in a 360 ton fiducial mass detector. To these, the absorption events must be added. For the same cut-off, using the ^8B neutrino flux from the Standard Solar Model [5b] and the capture cross-sections reported in ref [4b,c], the absorption reaction rates are 3.62 SNU and 1.68 SNU for Gamow-Teller and pure Fermi interactions respectively. This means 610 Gamow-Teller and 285 Fermi events per year. Scattering events occur with all types of neutrino flavours while absorption events occur with electron neutrino only. This is the reason why the triggers should be chosen in order to give the maximum discrimination between these two kinds of interactions.

5.1 Elastic events

It is very important to reconstruct for this kind of events the main vertex of the scattered electron. If this would not be the case, the background should be multiplied by a factor two. In our computations the first hit wire can be distinguished from the end point of one electron with an efficiency bigger than 80%. We choose as starting point of the electron the wire (between the two extreme hit wires) having the lower deposited energy. In fact the wire near the end point, due to multiple scattering increase, collects usually more charge than that one close to the main vertex.

We assume the following constraints as definition of the off-line trigger:

1) primary electron energy bigger than 5 MeV,

2) the cone aperture around the real emission direction of the electron is 25°, $(\text{efficiency } \alpha_1 = 0.65)$

3) associated multiplicity = 0 $(\text{efficiency } \alpha_2 = 0.81)$ (see Table I)

4) directionality requirement $(\text{efficiency } \alpha_3 = 0.80)$

The total detection efficiency $\alpha_{\text{elastic}} = \alpha_1 \cdot \alpha_2 \cdot \alpha_3 = 0.42$

The total elastic event expected rate will be about 140 /year.

The contamination of neutron capture events is 81% (see Table I) but the angular cut reduces this value to 4% of the background events. Hence we expect 25 background events/year in the shielded detector.

5.2 Gamow Teller events

We assume the following constraints as definition of the off-line trigger:

1) primary electron kinetic energy bigger than 5 MeV,

2) associated energy ≥ 1 MeV $(\alpha_{GT} = 0.69)$ (see Table II)

The final expectation will be about 422 events/year.

5.3 Fermi events

We assume the following constraints as definition of the off-line trigger:

1) primary electron kinetic energy bigger than 5 MeV,

2) associated energy ≥ 1 MeV $(\alpha_{\text{Fermi}} = 0.95)$ (see Table III)

The final expectation will be 270 event/year.

The total absorption rate will be 692 events/year with a contamination from neutron captures of 8.4% of the background events: 52 event/year.

We summarise the results in the following table, where the rates of events per year and per TPC chamber are shown, the background is written in parenthesis:

	TPC1	TPC2	TPC3	TPC4	TOTAL
Elastic channel (E≥5MeV) (background)	35 (13)	35 (3)	35 (2)	35 (7)	140 (25)
Elastic channel (E≥6MeV) (background)	30 (6)	30 (< 1)	30 (< 1)	30 (3)	120 (<11)
Absorption channels (background)	173 (28)	173 (6)	173 (4)	173 (14)	692 (52)

Tab. V Expected number of events per year compared with the rate of the computed noise. The four TPC are numbered from left to right looking the dewar from the entrance door. The numbers of events must be dumped by a factor ≅ 0.6, if we take into account the neutrino deficit revealed by experiments [15].

A 5.2% of Gamow Teller and 0.4% of Fermi type events can simulate elastic interactions. Keeping into account the angular cut this means a contamination of no more than 2 events/year in the elastic scattering sample.

A somewhat greater contamination from elastic into absorption sample is expected: i.e. 27 events/year.

From Table V we conclude that a clean measure of ^{8}B solar neutrinos can be performed in a reasonable data taking time. It is important to bear in mind that this is possible because of the low intensity of background signals. Noise is mainly related to the neutron flux level in LNGS laboratories and to the concentration of contaminants (especially uranium) in the materials which will be used for the detector construction. Little more can be done for what concerns neutron flux, but the choice of the materials must be accurate. Anyway purity requirements are within the values specified for industrial products which can easily be found on sale.

6. References

[1] a- Icarus Collaboration "ICARUS I : An optimised, real time detector of solar neutrinos" Internal report LNF - 89/005 (R) (1989)

b-"ICARUS II: second generation proton decay experiment and neutrino observatory at the Gran Sasso Laboratory" Proposal by the ICARUS Collaboration VOLUME I Internal report LNGS - 94/99-I May 1994.

c-"IICARUS II: second generation proton decay experiment and neutrino observatory at the Gran Sasso Laboratory" Proposal by the ICARUS Collaboration VOLUME II Internal report LNGS - 94/99-I May 1994.

d-"A search programme for explicit neutrino oscillations at long and medium baselines with ICARUS detector " Proposal by the ICARUS Collaboration Internal report ICARUS -TM-97/01 (5 March 1997).

[2] P.Cennini et al."A first 600 ton ICARUS detector installed at the Gran Sasso Laboratory" Proposal by the ICARUS Collaboration Addendum to proposal LNGS- 94/99 I & II May 1995.

[3] R.Bru, F.Bruyant, M.Maire, A.C.Mc Pherson and P.Zanarini GEANT 3, CERN report Data Handling Division, DD/EE/84-1, September 1987.

MCNP- A general Montecarlo code for neutron and photon transport Version 4.2 Los Alamos National Laboratory, LA7396-M, revised April 1991.

[4] (a) - J.N.Bahcall, M. Baldo-Ceolin, D.B. Cline and C.Rubbia, Phys. Lett. B 178 (1986) 324

(b) - W.E.Ormand, P.M.Pizzochero, P.F.Bortignon, and R.A.Broglia, "Gamow-Teller contributions to neutrino absorption cross sections for ^{40}Ar", Phys.Lett. B 345 (1995) 343.

(c) M.Bhattacharya et al. "Beta decay of ^{40}Ti and the efficiency of the ICARUS ^{40}Ar neutrino detector" internal report (April, 1997)

[5] a- J.N.Bahcall "Neutrino Physics" Cambridge University Press 1989, pag. 14,197,232.

b- J.N. Bahcall and M.H. Pinsonneault Rev. Mod. Phys. 64 (1992) 885, S.Turck-Chieze and I.Lopez Astrophys. Jour. 408 (1993) 347, N.Hata UPR-0612T and references therein.

[6] E. Bellotti, " Nuclear physics at Gran Sasso",Nuclear Physics News, vol. 1, n. 3, (1991)18

[7] Handbook of Chemistry and Physics, 46 ed, (1965)

[8] A. Esposito, "Misure di radioattivita' nei campioni di materiali da utilizzare per strutture interne del LNGS dell'INFN", LNF-86/60(R),1986

[9] R. Vandenbosch,J.R. Huizenga, "Nuclear Fission", Academic Press N.Y. (1973)

[10] J.B. Marion, J.L. Fowler,"Fast neutron physics", Interscience Publishers, N.Y.,(1960)

[11] P.Cennini et al. "On atmospheric ^{39}Ar and ^{42}Ar abundance" Nucl. Instr. and Methods A 356 (1994) 256.

[12] DBA Collaboration: data presented at LNGS Meeting (July 1997).

[13] C. Arpesella, S. Latorre, P.P. Sverzellati, LNGS 92/35 July 1992

[14] P. Belli et Al., "Deep underground neutron flux measurement with large BF3 counters", Il Nuovo Cimento, vol 101 A, n. 6 (1989),959

[15] - R.Davis et al., Proc. 21st Int. Cosmic Rays Conf., Univ. of Adelaide, ed. R.J.Protheroe, Vol. 12 (1990) 143, Proc. 23rd ICR, Calgary, Canada (1993), Prog. in Nucl. and Part. Phys. 32 (1994)
- GALLEX Coll. P.Anselmann et al. Phys. Lett. B285 (1992) 885, Phys. Lett. B388 (1996) 384
- Y.Suzuki Nucl. Phys. B (Proc. Suppl.) 35 (1994) 407, Nucl. Phys. B (Proc. Suppl.) 38 (1995) 54
- SAGE Coll. J.N.Abdurashitov et al. Phys. Lett. B328 (1994) 234, Nucl. Phys. B (Proc. Suppl.) 38 (1995) 60